Divergent Precursors of the Mott-Hubbard Transition at the Two-Particle Level

T. Schäfer,[1] G. Rohringer,[1] O. Gunnarsson,[2] S. Ciuchi,[3] G. Sangiovanni,[4] and A. Toschi[1]

[1]*Institute of Solid State Physics, Vienna University of Technology, 1040 Vienna, Austria*
[2]*Max Planck Institute for Solid State Research, D-70569 Stuttgart, Germany*
[3]*Dipartimento di Scienze Fisiche e Chimiche, Università dell'Aquila, and Istituto dei Sistemi Complessi, CNR, Via Vetoio I-67010 Coppito-L'Aquila, Italy*
[4]*Institut für Theoretische Physik und Astrophysik, Universität Würzburg, Am Hubland, D-97074 Würzburg, Germany*

(Received 4 March 2013; published 13 June 2013)

Identifying the fingerprints of the Mott-Hubbard metal-insulator transition may be quite elusive in correlated metallic systems if the analysis is limited to the single particle level. However, our dynamical mean-field calculations demonstrate that the situation changes completely if the frequency dependence of the two-particle vertex functions is considered: The first nonperturbative precursors of the Mott physics are unambiguously identified well inside the metallic regime by the divergence of the local Bethe-Salpeter equation in the charge channel. In the low-temperature limit this occurs for interaction values where incoherent high-energy features emerge in the spectral function, while at high temperatures it is traceable up to the atomic limit.

DOI: 10.1103/PhysRevLett.110.246405 PACS numbers: 71.27.+a, 71.10.Fd, 71.30.+h

Introduction.—Among all fascinating phenomena characterizing the physics of correlated electronic systems, one of the most important is undoubtedly the Mott-Hubbard metal-to-insulator transition (MIT) [1]. Here, the onset of an insulating state is a direct consequence of the strong Coulomb repulsion rather than the underlying electronic band structure. Mott MITs have been indeed identified in several correlated materials [2], especially in the class of transition metal oxides and heavy fermions. The interest in the Mott MIT is not limited, however, to the transition per se, but also includes the correlated (bad) metallic regime in its proximity. In fact, this region of the phase-diagram often displays a rich variety of intriguing or exotic phases, which are often related to the physics of the high-temperature superconducting cuprates.

An exact theoretical description of the Mott MIT represents a considerable challenge due to its intrinsically nonperturbative nature in terms of the electronic interaction. However, significant progress was achieved with the invention of the dynamical mean field theory (DMFT) [3,4]. By an accurate treatment of local quantum correlations, DMFT has allowed for the first nonperturbative analysis of the Mott-Hubbard MIT in the Hubbard model [5] and, in combination with *ab initio* methods [6], also for the interpretation and the prediction of experimental spectroscopic results for strongly correlated materials, such as, e.g., the paramagnetic phases of V_2O_3 [7]. Theoretically, the following "hallmarks" of the onset of the Mott insulating phase can be unambiguously identified in DMFT: At the one-particle level, a divergence of the local electronic self-energy in the zero-frequency limit is observed, reflecting the opening of the Mott spectral gap, while at the two-particle level, the local spin susceptibility ($\chi_s(\omega = 0)$) diverges at $T = 0$, due to the onset of long-living local magnetic moments in the Mott phase.

Description of the problem.—While the characterization of the MIT itself is quite clear, at least on a DMFT level, the physics of the correlated metal regime in the vicinity of the MIT is far from being trivial and presents several anomalies. We recall here the occurrence of kinks of purely electronic origin [8] in the angular resolved one-particle spectral functions or in the electronic specific heat, the formation of large instantaneous magnetic moments, screened by the metallic dynamics [9], the abrupt change of the out-of-equilibrium behavior after a quench of the electronic interaction [10], and the changes in the energy balance between the paramagnetic and the low-temperature (antiferromagnetically) ordered phase, which also affect the restricted optical sum rules [11]. Also motivated by these observations, many DMFT calculations focused on a general characterization of this regime, e.g., by studying the phase-diagram of the half-filled Hubbard model. However, no trace of other phase transitions has been found beyond the MIT itself and the (essentially) mean-field antiferromagnetically ordered phase, which is not of interest here. Hence, one of the main outcomes of the previous DMFT analyses, mostly focusing on the evolution of one-particle spectral properties (and, to a lesser extent, on susceptibilities [12]), has been the definition of the "borders" of the so-called crossover regions at higher T than those where the MIT can be observed. The shape of these crossover regions has been analyzed in many different ways [4,13–16]. We note here that the (different) criteria used for defining crossover regimes imply a certain degree of arbitrariness. Furthermore, the crossover region is located at much higher Ts than those where some of the above-mentioned anomalies are observed.

In this Letter, going beyond the standard, typically one-particle, DMFT analyses, we present a completely unambiguous criterion to distinguish the "weakly" and the "strongly" correlated regions in the phase diagram. By studying the frequency structure of the two-particle local vertex functions of DMFT, we observe the divergence of the local Bethe-Salpeter equation in the charge channel. This divergence defines a regime remarkably different, also in shape, from the crossover region, where nonperturbative precursor effects of the MIT become active, even well inside the low-temperature metallic phase. The precise definition of such a regime allows for a general interpretation of the anomalous physics emerging as a precursor of the MIT. Furthermore, our analysis, showing the occurrence of peculiar divergent features in some of the two-particle local vertex functions of DMFT is also expected to have a significant impact on future calculations for strongly correlated electron systems, because the two-particle local vertex functions represent a crucial ingredient for both (i) the calculation of dynamical momentum-dependent susceptibilities in DMFT [4,17,18], as well as (ii) the diagrammatic extensions [19,20] of the DMFT, aiming at the inclusion of nonlocal spatial correlations.

DMFT results at the two-particle level.—We consider the Hubbard model on a square lattice in the paramagnetic phase at half-filling, which is one of the most basic realizations of the MIT in DMFT. The corresponding Hamiltonian is

$$H = -t\sum_{\langle ij\rangle\sigma} c^{\dagger}_{i\sigma}c_{j\sigma} + U\sum_{i} n_{i\uparrow}n_{i\downarrow}, \qquad (1)$$

where t is the hopping amplitude between nearest neighbors, U is the local Coulomb interaction, and $c^{\dagger}_{i\sigma}(c_{i\sigma})$ creates (annihilates) an electron with spin $\sigma =\uparrow,\downarrow$ at site i; $n_{i\sigma} = c^{\dagger}_{i\sigma}c_{i\sigma}$. Hereafter, all energy scales will be given in units of $D = 4t = 1$, i.e., twice the standard deviation of the noninteracting DOS [21].

Differently from previous studies, we will focus on the analysis of the two-particle local vertex functions computed with DMFT. By using a Hirsch-Fye quantum Monte Carlo impurity solver [4], whose accuracy has been also tested in selected cases with exact-diagonalization DMFT calculations, we have first computed the generalized local susceptibility $\chi^{\nu\nu'}(\omega)$. This is defined, following the notation of Ref. [22], as

$$\chi^{\nu\nu'}_{\sigma\sigma'}(\omega) = \int d\tau_1 d\tau_2 d\tau_3 e^{-i\nu\tau_1} e^{i(\nu+\omega)\tau_2} e^{-i(\nu'+\omega)\tau_3} \times [\langle T_\tau c^{\dagger}_{\sigma}(\tau_1)c_{\sigma}(\tau_2)c^{\dagger}_{\sigma'}(\tau_3)c_{\sigma'}(0)\rangle - \langle T_\tau c^{\dagger}_{\sigma}(\tau_1)c_{\sigma}(\tau_2)\rangle\langle T_\tau c^{\dagger}_{\sigma'}(\tau_3)c_{\sigma'}(0)\rangle], \qquad (2)$$

where T_τ is the (imaginary) time-ordering operator and ν, ν' and ω denote the two fermionic and the bosonic Matsubara frequencies, respectively. Then, the Bethe-Salpeter equation in the charge channel [defined as $\chi^{\nu\nu'}_{c}(\omega) = \chi^{\nu\nu'}_{\uparrow\uparrow}(\omega) + \chi^{\nu\nu'}_{\uparrow\downarrow}(\omega)$] has been considered for $\omega = 0$, allowing us to determine the corresponding irreducible vertex [22]

$$\Gamma^{\nu\nu'}_{c} = [\chi^{\nu\nu'}_{c}(\omega = 0)]^{-1} - [\chi^{\nu\nu'}_{0}(\omega = 0)]^{-1}, \qquad (3)$$

where the last term is defined through the convolution of two DMFT Green's functions as $\chi^{\nu\nu'}_{0}(\omega) = -T^{-1}G(\nu)G(\nu+\omega)\delta_{\nu\nu'}$. The vertex $\Gamma^{\nu\nu'}_{c}$ can be viewed as the two-particle counterpart of the electronic self-energy and, for a half-filled system, it is a purely real function. Our numerical results are reported in Fig. 1 for four different values of the electronic interaction U at a fixed temperature of $T = 0.1$. Starting by examining the first panel, corresponding to the smallest value of $U = 1.2$, one observes two main diagonal structures in the Matsubara frequency space. These structures are easily interpretable as originated by reducible ladder processes in the (transverse) particle-hole ($\nu = \nu'$) and particle-particle ($\nu = -\nu'$) channels, respectively, [22]. Following the behavior of the local spin susceptibility in the Mott phase, the main diagonal structure will diverge exactly at the MIT ($U_{\mathrm{MIT}} \sim 3$) in the $T = 0$ limit [22,23].

In contrast to these standard properties of $\Gamma^{\nu\nu'}_{c}$, visible in the first panel, the analysis of the other three panels of Fig. 1 shows the emergence of a low-frequency singular behavior of the vertex functions for a value of U much smaller than that of the MIT. Already at $U = 1.27$ (second panel), one observes a strong enhancement of the vertex function at the lowest Matsubara frequencies (note the change in the intensity scale). This is visible as an emergent "butterfly"-shaped structure, where the intense red-blue color coding indicates alternating signs in the (ν, ν') space. Remarkably, such a low-energy structure becomes predominant over the other ones along the diagonals. That a true divergence takes place is suggested by the third panel ($U = 1.28$), where the intensity of the "butterfly" structure is equally strong, but the signs are now inverted as indicated by the colors. This is also shown more quantitatively by the values of $\Gamma^{\nu\nu'}_{c}$ along a selected path of $\Gamma^{\nu\nu'}_{c}$ in frequency space (lower panels in Fig. 1). Note that the inversion of the signs cannot be captured by second-order perturbation theory calculations (green circles), marking the nonperturbative nature of the result. The rigorous proof of the divergence is provided by the evolution of the matrix $\chi^{\nu\nu'}_{c}$, which is positive definite at weak coupling, while one of its eigenvalues (see legends and insets in the bottom row of Fig. 1) becomes negative crossing 0. Finally, by further increasing U, the low-energy structure weakens, indicating that at fixed $T = 0.1$ this vertex divergence is taking place only for a specific value of the Hubbard interaction, i.e., for $\tilde{U} \simeq 1.275$. This finding naturally leads to the crucial question of the temperature dependence of the results: Does such a divergence occur for all temperatures, and if yes, is the temperature dependence of $\tilde{U}$ significant? As one can immediately understand from Fig. 2, the answer to both

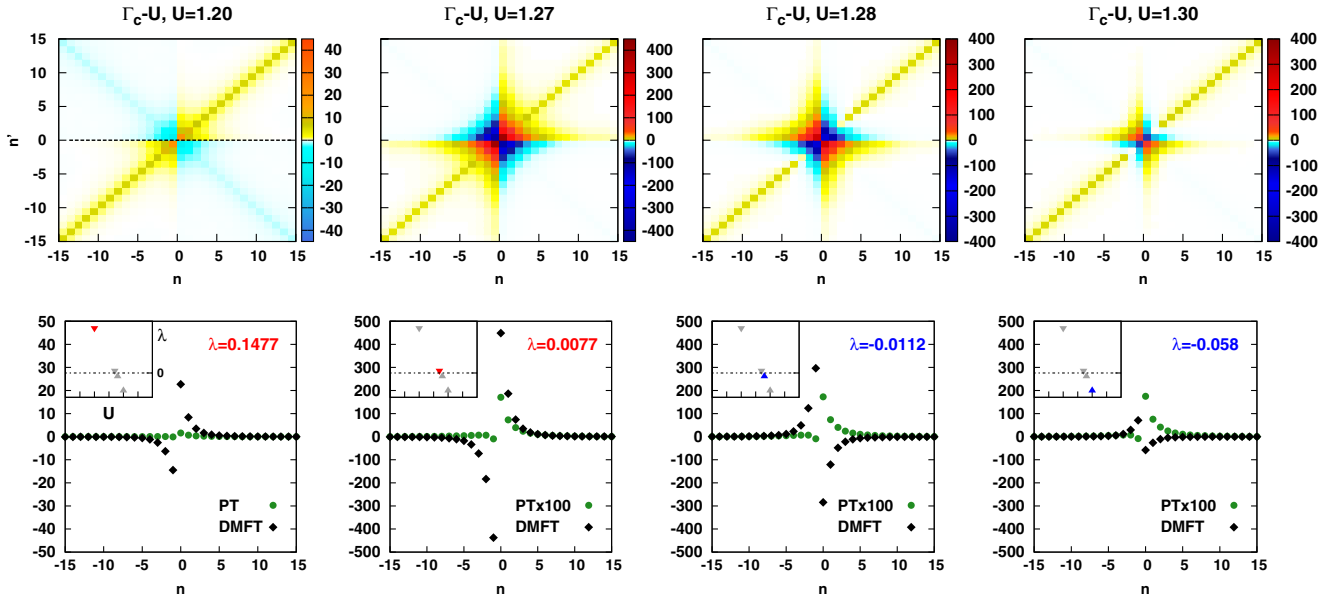

FIG. 1 (color online). *Upper row*: Evolution of the frequency-dependent two-particle vertex function, irreducible in the charge channel, ($\Gamma_c^{\nu\nu'}$) for increasing U. Note that the lowest-order contribution U has been always subtracted so that $\Gamma_c = U$ corresponds to the white color in all plots. The data have been obtained by DMFT at zero external frequency ($\omega = 0$) and fixed temperature ($T = 0.1$); *lower row*: linear snapshot of the same Γ_c along the path marked by the dashed line in the first panel of the upper row, i.e., as a function of $\nu = (\pi/\beta)(2n + 1)$ for $n' = 0$ ($\nu' = (\pi/\beta)$), compared to second-order perturbation theory (PT) results. In the legends/insets the closest-to-zero eigenvalue (λ) of $\chi_c^{\nu\nu'}/\chi_0^{\nu\nu'}$ is reported for each U.

questions is positive [24]. By repeating the analysis of Fig. 1 for different temperatures, we could identify the loci ($\tilde{T}$, $\tilde{U}$, red dots in Fig. 2) in the phase-diagram, where the low-frequency divergence of $\Gamma_c^{\nu\nu'}$ occurs. This defines a

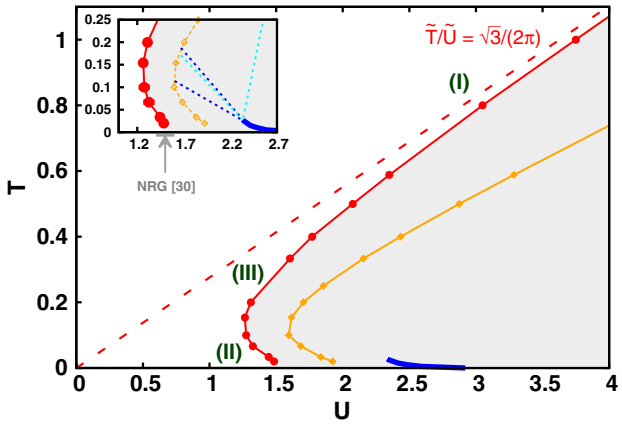

FIG. 2 (color online). Instability lines of the irreducible vertices in the charge (Γ_c red circles) and in the particle-particle channels (Γ_{pp} orange diamonds) reported in the DMFT phase diagram of the half-filled Hubbard model (the data of the MIT, blue solid line, are taken from Ref. [13,14]). The red dashed line indicates the corresponding instability condition ($\tilde{T} = (\sqrt{3}/2\pi)\tilde{U}$) estimated from the atomic limit. Inset: zoom on the low-T region, where also different estimations (dashed light blue [13], dashed blue [14]) of the crossover region are indicated [30].

curve $\tilde{T}(U)$ with a quite peculiar shape, where the following three regions can be distinguished: (I) at very high T, the behavior is almost perfectly linear $\tilde{T} \propto \tilde{U}$; (II) in the low T limit the curve strongly bends, extrapolating for $T \to 0$ at $\tilde{U}(0) \sim 1.5 \ll U_{\mathrm{MIT}} \sim 3$; (III) at intermediate T the curve interpolates between these two regimes, with a "reentrance" clearly affected by the presence of the MIT at larger U (blue line in Fig. 2). We note that by increasing U much further than the $\tilde{T}(U)$ curve, one eventually observes a divergence also of the local Bethe-Salpeter in the particle-particle channel (orange points in Fig. 2), while for all values of T, U considered, no similar divergence is found in the spin channel.

Interpretation of the results.—In contrast to the case of the main diagonal structures of the vertex functions, the interpretation of the low-frequency divergences of $\Gamma_c^{\nu\nu'}$ is not directly related to the MIT. However, even if at low T the divergences take place in the metallic region of the phase diagram, the reentrance shape of the $\tilde{T}(U)$ curve is indeed remarkably affected by the position of the MIT. The most natural interpretation is, hence, that the shaded area in the phase diagram defines the region where the precursor effects of the MIT physics preclude the perturbative description and become a crucial ingredient in determining the properties of the system. This interpretation is evidently supported by the fact that the signs of the two-particle vertex functions are correctly predicted in perturbation theory only up to the left-hand side of the $\tilde{T}(U)$ curve. More generally, the $\tilde{T}(U)$ curve can be

identified with the limit of the region of applicability of perturbative schemes based on the Baym-Kadanoff [25] functional $\Phi[G]$, since $(\delta^2\Phi/\delta G^2) = \Gamma_c$ can no longer be defined on that line. Note that this, in principle, does not preclude a generalized formulation of a Luttinger-Ward functional [26] also after having crossed the divergency line, hence preserving the conserving nature of the theory. At the same time, the low-frequency singularities of the vertex may render problematic the numerical evaluation of the Bethe-Salpeter equation to compute momentum-dependent DMFT response functions in specific regions of the phase diagrams, suggesting the use of alternative procedures [27].

As the singularity of Γ_c (and later on of Γ_{pp}) is not associated to simultaneous divergences in the other channels, the application of the local parquet equations [22,28] allows us to identify the ultimate root of these divergences in the fully two-particle irreducible diagrams. Hence, this is an "intrinsic" divergence, deeply rooted in the diagrammatics and not generated by ladder scattering processes in any channel. From a more physical point of view, the fact that the only irreducible vertex Γ displaying no singularities at low frequencies is the spin one, might also indicate the emergent role played by preformed local magnetic moments as MIT precursors, even in regions where the metallic screening is rather effective.

We can go, however, beyond these general considerations and analyze the three regimes of the $\tilde{T}(U)$ curve in detail, discussing the relation with the emergence of some of the anomalous properties of the physics in the vicinity of the MIT. The analysis of the high-T linear regime [(I) in Fig. 2] of $\tilde{T}(U)$ is probably the easiest. Here U, $T \gg D$, and hence a connection with the atomic limit ($D = 0$) can be established. Using analytic expressions [22,29] for the reducible two-particle vertex functions as an input for Eq. (3), we find that the low-frequency divergence of $\Gamma_c^{\nu\nu'}$ occurs at $\tilde{T}/\tilde{U} = (\sqrt{3}/2\pi)$ and that the eigenvector associated to the vanishing eigenvalue of $\chi_c^{\nu\nu'}$ has the particularly simple form, $(1/\sqrt{2})(\delta_{\nu(\pi T)} - \delta_{\nu(-\pi T)})$. As is clear from the comparison with the red dashed line in Fig. 2, this proportionality exactly matches the high-T linear behavior of our $\tilde{T}(U)$ curve. Crossing this curve in its high-T linear regime, which extends indeed over a large portion of the phase diagram, corresponds to entering a region where the thermal occupation of the high-energy doubly occupied or empty states becomes negligible, letting the physics be dominated by the local moments. The connection with the local moment physics also holds for the low-T region (II), though via a different mechanism. For $T \to 0$, the relevant energy scales are the kinetic ($\sim D$) and the potential (U) energy, whose competition is regulated by quantum fluctuations. In this case, obviously, only numerical results are available. We observe that the $T \to 0$ extrapolated value of $\tilde{U}(0) \sim 1.5$ falls in the same region (gray arrow in inset of Fig. 2), where DMFT(NRG) [30] see a first clear separation of the Hubbard subbands from the central quasiparticle peak ["dip" in the spectral function $A(\omega)$]. We recall here that the formation of well-defined minima in $A(\omega)$ between the central quasiparticle peak and the Hubbard subbands is directly connected with the anomalous phenomenon of the appearance of kinks in the electronic self-energy and specific heat [8]. At the same time, more recent DMFT(DMRG) [31] data rather indicate that for $U \geq \tilde{U}(0) \sim 1.5$ two sharp peak features emerge at the inner edges of the Hubbard subbands, which, however, would be already visible at $U \geq 1$.

Looking for a more analytical description of this scenario, we can consider the DMFT solution of the much simpler Falicov-Kimball (FK) model [32]. Here one can exactly show that $\Gamma_c^{\nu\nu'}$ indeed diverges before the MIT is reached (precisely at $\tilde{U}^{\mathrm{FK}} = (1/\sqrt{2})U_{\mathrm{MIT}}^{\mathrm{FK}}$). However, for the FK results, a direct relation with the formation of the two minima in $A(\omega)$ cannot be completely identified, as the renormalization of the central peak is not captured in this scheme [33]. Finally, in the intermediate temperature region (III), a direct connection with the structure of the spectral function or with the atomic physics cannot be made because here all the three energy scales (D, T, and U) are competing. However, an interesting observation can be made. Recent out-of-equilibrium calculations for the Hubbard model have shown [10] that after a quench of the interaction (i.e., from $U = 0$ to $U > 0$), the system's relaxation occurs in two different (nonthermal) ways. The changeover between these two regimes, however, appears for a given set of parameters, $\bar{U} \sim 1.65$ and $T_{\mathrm{eff}} \sim 0.4$, in close proximity of the vertex instability line in our phase diagram.

Conclusions and outlook.—Our DMFT calculations have shown how the emergent (nonperturbative) precursor effects of the MIT determine a low-frequency divergence of the local Bethe-Salpeter equation in the charge channel. This allows for an unambiguous identification of the regime, where perturbation and Baym-Kadanoff functional theory break down, and where, at the same time, several anomalous properties are observed or predicted for correlated metals. Taking properly into account the physics emerging from the singularity of the two-particle vertex functions will represent one of the main challenges for future improvements of the theoretical many-body treatments at the precision level required by the increasingly high experimental standards.

T. S., G. R., and A. T. acknowledge financial support from the Austrian Science Fund (FWF) through Project No. I610-N16. Numerical calculations have been performed on the Vienna Scientific Cluster (VSC) and at the MPI-FKF in Stuttgart. We thank for insightful discussions M. Capone, K. Held, A. Georges, A. Katanin, C. Castellani, M. Fabrizio, H. Hafermann, E. Gull, E. Kozik, J. Kuneš, S. Andergassen, A. Valli, and C. Taranto. We thank P. Thunström for showing us his density-matrix renormalization group (DMRG) DMFT data. G. S. acknowledges financial support from the DFG (FOR 1346).

[1] N. F. Mott, Rev. Mod. Phys. **40**, 677 (1968); *Metal-Insulator Transitions* (Taylor & Francis, London, 1990); F. Gebhard, *The Mott Metal-Insulator Transition* (Springer, Berlin, 1997).

[2] M. Imada, A. Fujimori, and Y. Tokura, Rev. Mod. Phys. **70**, 1039 (1998).

[3] W. Metzner and D. Vollhardt, Phys. Rev. Lett. **62**, 324 (1989); A. Georges and G. Kotliar, Phys. Rev. B **45**, 6479 (1992).

[4] A. Georges, G. Kotliar, W. Krauth, and M. J. Rozenberg, Rev. Mod. Phys. **68**, 13 (1996).

[5] J. Hubbard, Proc. R. Soc. A **276**, 238 (1963).

[6] G. Kotliar, S. Savrasov, K. Haule, V. Oudovenko, O. Parcollet, and C. Marianetti, Rev. Mod. Phys. **78**, 865 (2006); K. Held, Adv. Phys. **56**, 829 (2007).

[7] K. Held, G. Keller, V. Eyert, D. Vollhardt, and V. I. Anisimov, Phys. Rev. Lett. **86**, 5345 (2001); A. I. Poteryaev, J. Tomczak, S. Biermann, A. Georges, A. Lichtenstein, A. Rubtsov, T. Saha-Dasgupta, and O. Andersen, Phys. Rev. B **76**, 085127 (2007); P. Hansmann, A. Toschi, G. Sangiovanni, T. Saha-Dasgupta, S. Lupi, M. Marsi, and K. Held, Phys. Status Solidi B, 1 (2013).

[8] K. Byczuk, M. Kollar, K. Held, Y.-F. Yang, I. A. Nekrasov, Th. Pruschke, and D. Vollhardt, Nat. Phys. **3**, 168 (2007); A. Toschi, M. Capone, C. Castellani, and K. Held, Phys. Rev. Lett. **102**, 076402 (2009).

[9] A. Toschi, R. Arita, P. Hansmann, G. Sangiovanni, and K. Held, Phys. Rev. B **86**, 064411 (2012).

[10] M. Eckstein, M. Kollar, and P. Werner, Phys. Rev. Lett. **103**, 056403 (2009); M. Schirò and M. Fabrizio, Phys. Rev. B **83**, 165105 (2011).

[11] C. Taranto, G. Sangiovanni, K. Held, M. Capone, A. Georges, and A. Toschi, Phys. Rev. B **85**, 085124 (2012); A. Toschi, M. Capone, and C. Castellani, Phys. Rev. B **72**, 235118 (2005).

[12] C. Raas and G. S. Uhrig, Phys. Rev. B **79**, 115136 (2009).

[13] R. Bulla, Phys. Rev. Lett. **83**, 136 (1999).

[14] N. Blümer, Ph.D thesis, Augsburg, 2003.

[15] S. Ciuchi, G. Sangiovanni, and M. Capone, Phys. Rev. B **73**, 245114 (2006).

[16] H. Terletska, J. Vucicevic, D. Tanaskovic, and V. Dobrosavljevic, Phys. Rev. Lett. **107**, 026401 (2011).

[17] J. Kuneš, Phys. Rev. B **83**, 085102 (2011).

[18] H. Park, K. Haule, and G. Kotliar, Phys. Rev. Lett. **107**, 137007 (2011).

[19] A. Toschi, A. A. Katanin, and K. Held, Phys. Rev. B **75**, 045118 (2007); G. Rohringer, A. Toschi, A. Katanin, and K. Held, Phys. Rev. Lett. **107**, 256402 (2011).

[20] A. N. Rubtsov, M. I. Katsnelson, and A. I. Lichtenstein, Phys. Rev. B **77**, 033101 (2008); H. Hafermann, G. Li, A. Rubtsov, M. Katsnelson, A. Lichtenstein, and H. Monien, Phys. Rev. Lett. **102**, 206401 (2009).

[21] As in DMFT the kinetic energy scale is controlled by D, DMFT results for different DOSes will present only minor differences provided that the value of U/D is the same. This is particularly true in the nonperturbative regime we are going to focus on in the following.

[22] G. Rohringer, A. Valli, and A. Toschi, Phys. Rev. B **86**, 125114 (2012).

[23] J. Bauer and A. C. Hewson, Phys. Rev. B **81**, 235113 (2010).

[24] In the Appendix of arXiv:1104.3854v1, a two-particle vertex divergence was also reported (for one temperature) whose position would be controlled by U rather than by T. This expectation is, however, not verified by our data of Fig. 2.

[25] G. Baym and L. P. Kadanoff, Phys. Rev. **124**, 287 (1961).

[26] M. Potthoff, Condens. Matter Phys. **9**, 557 (2006).

[27] N. Lin, E. Gull, and A. J. Millis, Phys. Rev. Lett. **109**, 106401 (2012).

[28] D. Senechal *et al.*, in *Theoretical Methods for Strongly Correlated Electrons* (Springer, New York, 2003), chap. 6.

[29] H. Hafermann, C. Jung, S. Brener, M. I. Katsnelson, A. N. Rubtsov, and A. I. Lichtenstein, Europhys. Lett. **85**, 27 007 (2009); S. Pairault, D. Sénéchal, and A.-M. S. Tremblay, Eur. Phys. J. B **16**, 85 (2000).

[30] R. Zitzler, Ph.D. thesis (Augsburg, 2004); R. Bulla, Phys. Rev. Lett. **83**, 136 (1999), we thank also R. Bulla for making the raw numerical renormalization group (NRG) data available to K. Held and his group.

[31] M. Karski, C. Raas, and G. S. Uhrig, Phys. Rev. B **77**, 075116 (2008).

[32] J. K. Freericks and V. Zlatić, Rev. Mod. Phys. **75**, 1333 (2003).

[33] Note that the DMFT solution of the FK model, coinciding with the CPA, can only capture the MIT via a rigid separation of the Hubbard band. Here the formation of a central minimum occurs already at $U = (1/2)U_{\mathrm{MIT}}^{\mathrm{FK}}$.